







Design and Analytical Studies of a DLC Thin-Film Piezoresistive Pressure Microsensor

Luiz Antonio Rasia¹ , Gabriela Leal² ,
Leandro Léo Koberstein³ , Humber Furlan⁴ , Marcos Massi⁵ ,
and Mariana Amorim Fraga⁶ 

¹ Universidade Regional do Noroeste do Estado do Rio Grande do Sul,
Ijuí, Brazil

rasia@unijui.edu.br

² Universidade Federal de São Paulo, São José dos Campos, Brazil

gabriela.leal@unifesp.br

³ Faculdade de Tecnologia de São José dos Campos,
São José dos Campos, Brazil

lleok@uol.com.br

⁴ Faculdade de Tecnologia de São Paulo, São Paulo, Brazil

humber@fatecsp.br

⁵ Universidade Presbiteriana Mackenzie, São Paulo, Brazil

massi.marcos@gmail.com

⁶ Universidade Brasil, São Paulo, Brazil

mafraga@ieee.org

Abstract. Diamond-like carbon (DLC) thin films have been investigated for a wide range of applications due to their excellent electrical and mechanical properties. In the last decade, several researches and development activities have been conducted on the use of these thin films as piezoresistors in MEMS pressure sensors. This paper provides an overview on the design of a piezoresistive pressure sensor constituted of a silicon circular diaphragm with four DLC thin-film piezoresistors arranged in the Wheatstone bridge configuration. The sensor was designed from analytical formulas found in the literature.

Keywords: Piezoresistive pressure sensor · Diamond-like carbon (DLC) · Design · Analytical solution

1 Introduction

Piezoresistive semiconductor sensors based on micro-electro-mechanical systems (MEMS) technology have superior performance compared to many conventional sensors in terms of sensitivity, stability, resolution and size. However, harsh-environment sensing measurements have some significant technical challenges to overcome; among them is the development of stable and functional materials to withstand extreme temperatures and corrosive media [1]. In these hard conditions, traditional semiconductor sensors typically exhibit low performance, which is mainly associated to their material properties and packaging technology [2].

Silicon is the most common semiconductor material used in MEMS piezoresistive sensors. These devices due to physical and electronic properties of the silicon, such as small bandgap energy (1.12 eV), have application limited in harsh environments, particularly at high temperatures. The literature shows that at higher temperatures silicon undergoes creep under minimal load which makes it unsuitable for sensor applications. In addition, it has relatively low values for its Young's modulus, hardness and its fracture toughness [1, 3].

The factors mentioned above have motivated studies on synthesis and processing of different material types (semiconductors, polymers and metals) to replace the silicon in MEMS, especially as sensing material. Carbon-based materials, such as diamond, diamond-like carbon (DLC) and silicon carbide (SiC), are recognized as the promising materials because they possess excellent physical properties that silicon and other materials lack. The excellent electrical, mechanical and thermal properties of carbon-based materials made them an obvious choice for microelectronics device and MEMS sensor applications. These materials exhibit very high Young's modulus, high tensile and fracture strength associated to good piezoresistive properties [4].

The focus of this paper is on the use of DLC thin films as piezoresistive sensing materials. Piezoresistive effect has been shown fundamental in MEMS sensing. The sensitivity of the sensors based in this effect is known as gauge factor (GF) and is defined by:

$$GF = \frac{\Delta R/R}{\varepsilon} \quad (1)$$

Where $\Delta R/R$ is the normalized resistance variation; ε is the mechanical strain.

The electrical resistance R can be written as:

$$R = \frac{\rho \cdot L}{A} \quad (2)$$

where ρ is the electrical resistivity t of the material; L and A are geometric parameters of the resistor (length and the cross-sectional, respectively). This equation can also be written as:

$$R = \frac{\rho \cdot L}{wt} \quad (3)$$

where w is the width and t is the thickness of the resistor.

Based on the orientation of the resistor, the gauge factors can be divided into longitudinal (GF_L) and transverse gauge (GF_T) factors as follows:

$$GF = \frac{\Delta R_L/R}{\varepsilon_L} \quad (4)$$

$$GF = \frac{\Delta R_T/R}{\varepsilon_T} \quad (5)$$

where ΔR_L and ΔR_T are the changes in resistance when the resistors are placed longitudinally and transversely to the applied strain, respectively. The component of strain in the longitudinal direction (ε_L) can be expressed as ratio of change in length to the initial length:

$$\varepsilon_L = \frac{\Delta L}{L} \quad (6)$$

Hooke's law relates the strain longitudinal to the stress (σ) as follows:

$$\sigma = E\varepsilon_L \quad (7)$$

where E is the Young's modulus or the modulus of elasticity of the material.

The transverse strain (ε_T) is proportional to the longitudinal strain (ε_L) within the range of Hooke's law. Hence, the negative ratio of these components is called Poisson's ratio (ν) and can be written as:

$$\nu = -\frac{\varepsilon_T}{\varepsilon_L} \quad (8)$$

Differentiating Eq. (3):

$$\frac{\partial R}{R} = \frac{\partial \rho}{\rho} + \frac{\partial L}{L} - \frac{\partial w}{w} - \frac{\partial t}{t} \quad (9)$$

Therefore, the resistance changes can also be expressed, in two directions when longitudinal and transverse strain is applied respectively as:

$$\frac{\partial R_L}{R} = \frac{\partial \rho}{\rho} + \varepsilon_L + \nu\varepsilon_L + \nu\varepsilon_L = \frac{\partial \rho}{\rho} + (1 + 2\nu).\varepsilon_L \quad (10)$$

$$\frac{\partial R_T}{R} = \frac{\partial \rho}{\rho} - \nu\varepsilon_T - \varepsilon_T + \nu\varepsilon_T = \frac{\partial \rho}{\rho} - \varepsilon_T \quad (11)$$

The choice of a piezoresistive material to develop the piezoresistive sensor is based on the desirable characteristics of the device, such as sensitivity (gauge factor value), nominal electrical resistance, thermal coefficient of resistance (TCR), temperature coefficient of gauge factor (TCGF) and stability.

1.1 Properties of DLC Thin Films

The three possible carbon hybridizations (sp^1 , sp^2 and sp^3), which are shown in Fig. 1, make carbon unique due to its various allotropes. Diamond is one of its allotropes and has only sp^3 bond hybridizations. Because of its atomic arrangement, diamond presents high hardness, high electrical resistivity and low wear rate among other properties. Meanwhile the graphite that has only sp^2 bond hybridization presents low hardness, low electrical resistivity and high wear rate [5]. Diamond-like carbon (DLC) is another

carbon allotrope that presents both hybridizations: sp^3 and sp^2 . This configuration gives the DLC unique properties, merged between diamond and graphite properties, such as high mechanical hardness, chemical inertness, optical transparency and wide band gap [6]. Table 1 compares the properties of DLC and diamond.

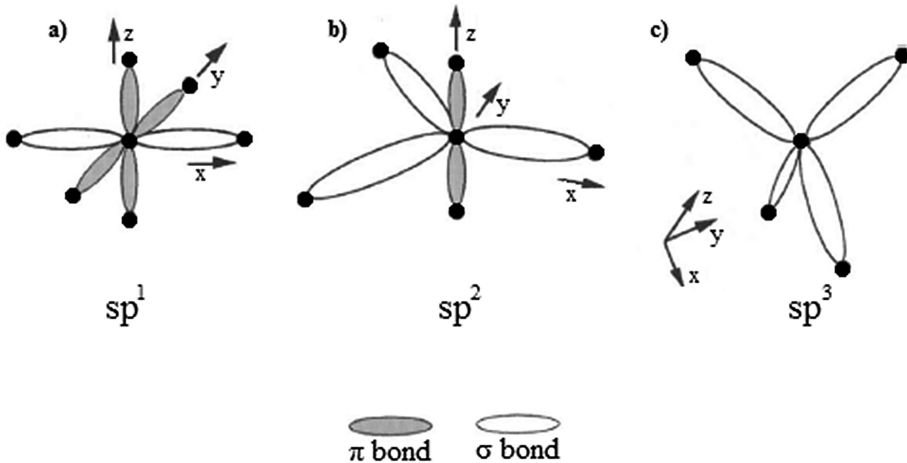


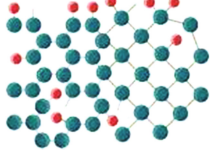
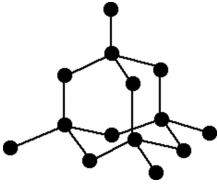
Fig. 1. Schematic representation of carbon hybridizations: (a) sp^1 , (b) sp^2 and (c) sp^3 (adapted from [7])

According to Robertson the sp^1 configuration consists in two of the four electrons forming σ bond along x axis and the other two electrons lies in a $p\pi$ orbital in y and z directions [6]. While in sp^2 three of four electron form σ bonds in a plane and the fourth electron lies in a $p\pi$ -orbital and in sp^3 each of four electrons form a strong σ bond to adjacent in a tetrahedral configuration. The extreme physical properties of diamond come from its strong directional σ bonds. Thus, the physical properties of DLC depend on the quantity of sp^2 and sp^3 bonds presents in this material.

In Table 1 it can be observed the major properties of amorphous carbon and other carbon materials compared with the quantity of sp^3 bond and hydrogen. The term DLC was used for the first time in 1971 by Aisenberg and Chabot [9], but a variety of names has been used to differentiate the types of DLC. The term a-C is used to all of amorphous carbon materials with a medium portion (40–60%) of sp^3 bonds while ta-C term (tetrahedral carbon) is used to carbon materials with high sp^3 concentration (more than 70%). The prefix :H is used to indicate that the material is hydrogenated while hydrogen free DLC don't receive this prefix. Some authors choose the use of a-C and ta-C rather than DLC or even the use of other variations as TAC (tetrahedral amorphous carbon) and others [7].

Therefore, as mentioned previously, the properties of DLC depend largely on the amount of sp^2 and sp^3 bonds and of the hydrogen content in the material, being that the mechanical properties depend on these three factors, except the elastic modulus and

Table 1. Summary of the properties of DLC and diamond (adapted from [8]).

Properties	DLC	Diamond
Structural	Amorphous (mixture of sp^2 (graphite) and sp^3 (diamond)) 	Cubic structure 
Physical	<ul style="list-style-type: none"> • Low thermal expansion coefficient • Thermal conductivity at room temperature ($100\text{--}700 \text{ W m}^{-1} \text{ K}^{-1}$) • Dielectric constant (3.0–6.0) 	<ul style="list-style-type: none"> • High melting point ($\sim 4000 \text{ }^\circ\text{C}$) • Low thermal expansion coefficient at room temperature ($1 \times 10^{-6} \text{ K}^{-1}$) • High thermal conductivity at room temperature ($2000 \text{ W m}^{-1} \text{ K}^{-1}$) • Low dielectric constant (5.7)
Electronic	<ul style="list-style-type: none"> • Bandgap (0.8–4.0 eV) • Wide range of electrical resistivities ($10^2\text{--}10^{12} \text{ } \Omega\cdot\text{cm}$) • High electric breakdown field ($>2.5 \text{ MV/cm}$) 	<ul style="list-style-type: none"> • Wide bandgap (5.45 eV, indirect gap) • High electrical resistivity ($10^{13}\text{--}10^{16} \text{ } \Omega\cdot\text{cm}$) • High saturated electron velocity ($2.7 \times 10^7 \text{ cm/s}$) • High electric breakdown field (10 MV/cm)
Mechanical	<ul style="list-style-type: none"> • Hardness (40–60 GPa) • High Young's modulus (200–750 GPa) • Excellent tribological properties • Potential solid lubricant coating 	<ul style="list-style-type: none"> • High hardness ($\sim 90 \text{ GPa}$) and wear resistance • High Young's modulus ($\sim 1050 \text{ GPa}$) • High strength/ tensile ($>1.2 \text{ GPa}$) • Low compressibility ($8.3 \times 10^{-3} \text{ m}^2 \text{ N}^{-1}$)
Optical	<ul style="list-style-type: none"> • High refractive index (1.8–3.0) • Low reflectance • Anti-reflective and scratch resistant coatings for IR optics 	<ul style="list-style-type: none"> • High refractive index (2.41) • Optical transparency • (UV to far IR) • Highly resistant to damage from irradiation
Chemical	<ul style="list-style-type: none"> • Chemical inertness • Excellent coating material for medical implants 	<ul style="list-style-type: none"> • High resistance to corrosion • Chemically and biologically inert

hardness that depend only on the sp^3 bonds. Meanwhile the electronic properties depend on the fraction and configuration of sp^2 bonds.

According to Takeno et al., although DLC has attractive mechanical properties in order to use this material in sensors, it is necessary to improve its electrical functionality control by light element or metal doping [10]. Characteristics such as electrical resistivity and TCR can be improved by the addition of metal in DLC matrix, forming Me-DLC films [11, 12].

It is known that a wide range of properties can be achieved by varying the synthesis process of DLC. However, DLC is always a thin film, not a bulk [13]. In your paper, Robertson explains that DLC occurs by deposition from energetic ion beams of carbon ions, created by the graphite sputtering or by the formation of an arc from a graphite target, or of hydrocarbon ions created by a discharge or plasma formed in a hydrocarbon gas or by sputtering graphite in hydrogen-containing atmosphere [13].

Currently, PVD (Physical Vapor Deposition) and CVD (Chemical Vapor Deposition) processes are the most used to deposit DLC films. Magnetron sputtering and cathodic vacuum arc are most used PVD techniques. In these techniques, physical processes (ionic impingement on a target and evaporation, respectively) are responsible for the atoms transfer from the source to the substrate [14]. While that, PECVD is the main CVD technique. In this process, the reaction between the precursor gases is stimulated or activated by the plasma [15].

1.2 Piezoresistive Sensors Based on DLC Thin Films

According to Takeno et al. the strain dependence of normalized resistance can be defined by [10]:

$$\frac{\Delta R}{R} = K \cdot \varepsilon \quad (12)$$

Where ΔR is the difference between the resistance with an applied strain and the resistance without strain, ε is strain and k is the gauge factor which can be expressed as:

$$K = 1 + 2\sigma + \pi E \quad (13)$$

Where σ is Poisson ratio, E is Young's module and π is piezoresistive coefficient. Since in metals the effect for the variation of resistance against the strain is small, its piezoresistive coefficient is close to zero, because that they exhibit low GF values (generally between 2 and 4) [16]. However, semiconductor materials present a strong variation in resistivity following a deflection, which result in a gauge factor generally higher than metals [17].

In 1999, Luethje and Brand observed the piezoresistive properties of DLC and Me-DLC thin films [18]. In 2006, Peiner et al. reported for the first time a study of piezoresistive properties of amorphous carbon strain gauges integrated in a silicon cantilever. The gauge factor of a-C films was determined by deflecting the cantilever and measuring the resistance change at compressive and tensile strains as well as under longitudinal and transversal conditions. They concluded that a-C films, besides having favorable mechanical properties, also showed a large piezoresistive effect with the gauge factor varying from 37 to 46 [19]. In the same year, a study comparing the piezoresistive properties among the aforementioned a-C film with an a-C:H thin film deposited by PECVD was reported by Tibrewala et al. [20]. The GF measurements of the a-C:H films were conducted using a test structure based on a silicon boss membrane. It was obtained GF values from 100 to 1200. Fraga et al. have found a GF around 70 for sputtered DLC films [21].

2 Design and Analytical Studies of the Pressure Sensor

The purpose is developing a piezoresistive pressure sensor constituted of a circular monocrystalline silicon diaphragm with four DLC thin-film piezoresistors arranged in the Wheatstone bridge configuration as shows Fig. 2. This layout allows using the benefits of DLC as sensing elements associated to well-known silicon microfabrication technologies to form the diaphragm by deep plasma etching. The sensor structure will be fully to design by analytical solution.

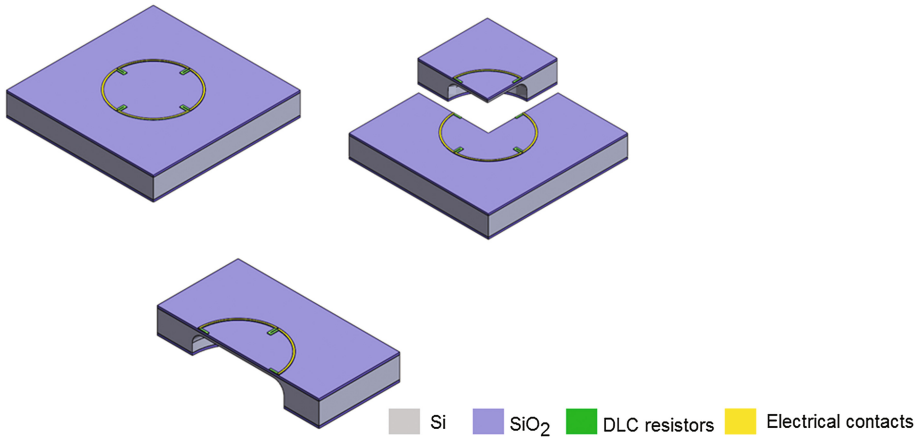


Fig. 2. Schematic representation of the pressure sensor

Kanda and Yasukawa demonstrated that the maximum stress of the square diaphragm is 1.64 times as large as that of the circular diaphragm when their diaphragm thickness is the same, i.e. the square diaphragm exhibits better characteristics than a circular [22]. However, from the fabrication viewpoint, the progress in plasma etching technology of silicon has become the circular diaphragm attractive to replace KOH etching.

2.1 Silicon Circular Diaphragm

Thin plate or small deflection theory is often used, and is appropriate for deflections less than 1/5 of the diaphragm thickness [3]. The maximum deflection, w_{max} , of a clamped circular plate under a uniform applied pressure is given by:

$$w_{max} = \frac{3(1-\nu)^2 p r^4}{16 E t^3} \quad (14)$$

Where E is Young's modulus, ν is Poisson's ratio, p is the applied pressure, r and t are, respectively, the radius and the thickness of the circular plate. The small deflection theory determines that:

$$w_{max} \leq \frac{1}{5}t \quad (15)$$

Substituting the Eq. (14) in (15):

$$\left(\frac{r}{t}\right)^4 \leq \frac{16E}{15p(1-v^2)} \quad (16)$$

The material of the diaphragm was considered to be silicon with $E = 180$ GPa and $v = 0.18$. A uniform pressure of 100 kPa was applied to the entire surface of the circular diaphragm. Therefore,

$$\frac{r}{t} \leq 37.5 \quad (17)$$

2.2 DLC Thin-Film Resistors

The piezoresistive effect relates the change in electrical resistance of the resistor as a function of the material piezoresistive coefficient and of the longitudinal stress as follows:

$$\frac{\Delta R}{R} = \sigma_l \pi_l \quad (18)$$

Where π_l is the longitudinal piezoresistive coefficient and the maximum longitudinal stress which is given by

$$\sigma_l = \frac{3pr^2}{4t^2} \quad (19)$$

Substituting the Eq. (19) in (18):

$$\frac{\Delta R}{R} = \frac{3}{4} \pi_l p \left(\frac{r}{t}\right)^2 \quad (20)$$

It is known that the piezoresistive coefficients are sensitive to several quantities such as conductivity type, orientation, temperature and doping level [4]. In this work, we consider the longitudinal piezoresistive coefficient of undoped DLC film ($\pi_l = 2.3 \times 10^{-10}$) [23]. Therefore,

$$\frac{\Delta R}{R} = 1.725 \cdot 10^{-5} \left(\frac{r}{t}\right)^2 \quad (21)$$

Substituting the Eq. (21) in (17):

$$\frac{\Delta R}{R} \leq 0.024 \quad (22)$$

The expressions (17) and (22) determine the maximum values for (r/t) and $(\Delta R/R)$ respectively. Figure 3 shows $(\Delta R/R)$ as function of (r/t) . As the objective is the development of a small sensor with good sensitivity. For this reason, we have selected $(r/t) = 25$. Therefore, the sensor presents circular diaphragm with $r = 500 \mu\text{m}$ and $t = 20 \mu\text{m}$.

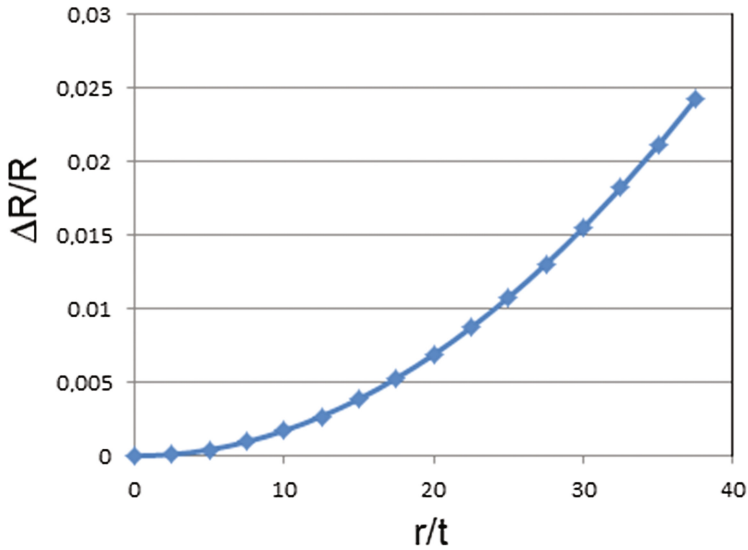


Fig. 3. The fractional change of resistance as a function of (r/t) .

3 Conclusions

The benefits of use DLC thin-film resistors in piezoresistive pressure sensors were presented. In addition, we describe a simple and efficient methodology for design a pressure sensor with silicon circular diaphragm using only analytical formulas found in the literature. Using this methodology, it is possible to design the sensor for different pressure ranges.

Acknowledgments. São Paulo Research Foundation – FAPESP (processes number 14/18139-8 and 13/17045-7) and by CNPq (processes number 442133/2014-6 and 305153/2015-3).

References

1. Fraga, M.A., Pessoa, R.S., Massi, M., Maciel, H.S.: Silicon carbide as base material for MEMS sensors of aerospace use: an overview. *Matéria* **19**(3), 274–290 (2014)
2. Casady, J.B., Johnson, R.W.: Status of silicon carbide (SiC) as a wide-bandgap semiconductor for high-temperature applications: a review. *Solid-State Electron.* **39**(10), 1409–1422 (1996)
3. Auciello, O., Pacheco, S., Sumant, A.V., Gudeman, C., Sampath, S., Datta, A., Carpick, R. W., Adiga, V.P., Zurcher, P., Ma, Z., Yuan, H.-C., Carlisle, J.A., Kabius, B., Hiller, J., Srinivasan, S.: Are diamonds a MEMS' best friend? *IEEE Microw. Mag.* **8**(6), 61–75 (2007)
4. Fraga, M.A., Furlan, H., Pessoa, R.S., Massi, M.: Wide bandgap semiconductor thin films for piezoelectric and piezoresistive MEMS sensors applied at high temperatures: an overview. *Microsyst. Technol.* **20**, 9–21 (2014)
5. Vetter, J.: 60 years of DLC coatings: historical highlights and technical review of cathodic arc processes to synthesize various DLC types, and their evolution for industrial applications. *Surf. Coat. Technol.* **257**, 213–240 (2014)
6. Robertson, J.: Diamond-like amorphous carbon. *J. Mater. Sci. Eng. R.* **37**, 129–281 (2002)
7. Silva, S.R.E., Carey, J.D.: Amorphous carbon thin films. In: Nalwa, H.S. (ed.) *Handbook of Thin Films*, vol. 4, pp 403–506. Elsevier Inc., Burlington (2002)
8. Fraga, M.A., Bosi, M., Negri, M.: Silicon Carbide in microsystem technology – thin film versus bulk material. In: Sadow, S.E., La Via, F. (eds.) *Advanced Silicon Carbide Devices and Processing*, pp. 1–30. Intech (2015)
9. Aisenberg, S., Chabot, R.: Ion-beam deposition of thin films of diamond like carbon. *J. Appl. Phys.* **42**(7), 2953–2958 (1971)
10. Takeno, T., Miki, H., Sugawara, T., Hoshi, Y., Takagi, T.: A DLC/W-DLC multilayered structure for strain sensing applications. *Diam. Relat. Mater.* **17**(4–5), 713–716 (2008)
11. Petersen, M., Heckmann, U., Bandorf, R., Gwozdz, V., Schnabel, S., Bräuer, G., Klages, C. P.: Me-DLC films as material for highly sensitive temperature compensated strain gauges. *Diam. Relat. Mater.* **20**(5–6), 814–818 (2011)
12. Leal, G., Fraga, M.A., Rasia, L.A., Massi, M.: Impact of high N₂ flow ratio on the chemical and morphological characteristics of sputtered N-DLC films. *Surf. Interface Anal.* **49**(2), 99–106 (2017)
13. Robertson, J.: Diamond-like carbon films, properties and applications. In: Sarin, V.K. (ed.) *Comprehensive Hard Materials*, vol. 3, pp. 101–139. Elsevier Inc., Burlington (2014)
14. Freund, L.B., Suresh, S.: *Thin Film Materials: Stress, Defect Formation and Surface Evolution*, pp. 1–820. Cambridge University Press, Cambridge (2003)
15. Martin, P.M.: *Handbook of Deposition Technologies for Films and Coatings Third Edition. Science Applications and Technology*. Elsevier Inc., Burlington (2010)
16. Kenny, T.: Strain gages. In: Wilson, J.S. (eds.) *Sensor Technology Handbook*, Elsevier Inc., Burlington, pp. 501–529 (2005)
17. Russo, G.P.: *Aerodynamic Measurement: From Physical Principles to Turnkey Instrumentation*, pp. 1–24. Woodhead Publishing, Elsevier Inc., Burlington (2011)
18. Luethje, H., Brand, J.: German Patent DE 199 54 164 A1. Sensor zur Zustandsbestimmung von Kenngrößen an mechanischen Komponenten (1999)
19. Peiner, E., Tibrewala, A., Bandorf, R., Biehl, S., Lüthje, H., Doering, L.: Micro force sensor with piezoresistive amorphous carbon strain gauge. *Sens. Actuators A: Phys.* **130–131**, 75–82 (2006)

20. Tibrewala, A., Peiner, E., Bandorf, R., Biehl, S., Lüthje, H.: Transport and optical properties of amorphous carbon and hydrogenated amorphous carbon films. *Appl. Surf. Sci.* **252**(15), 5387–5390 (2006)
21. Fraga, M.A., Furlan, H., Pessoa, R.S., Rasia, L.A., Mateus, C.F.R.: Studies on SiC, DLC and TiO₂ thin films as piezoresistive sensor materials for high temperature application. *Microsyst. Technol.* **18**, 1027–1033 (2012)
22. Kanda, Y., Yasukawa, A.: Optimum design considerations for silicon piezoresistive pressure sensors. *Sens. Actuators A* **62**, 539–542 (1997)
23. Geremias, M., Moreira, R.C., Rasia, L.A., Moi, A.: Mathematical modeling of piezoresistive elements. *J. Phys: Conf. Ser.* **648**, 012012 (2015)